Biointerface Research in Applied Chemistry
Open-Access Journal (ISSN: 2069-5837)

Article
Volume 13, Issue 2, 2023, 152
https://doi.org/10.33263/BRIAC132.152

Structural Stability and Electronic Properties of 2D MXene $Hf_3C_2F_2$ Monolayer by Density Functional Theory Approach

Rahulkumar P. Jadav [1], Pushkar Mishra [1], Sandip Kumavat [1], Deobrat Singh [2], Rajeev Ahuja [3], Yogesh Sonvane [1,*]

[1] Advanced Materials Lab, Department of Physics, Sardar Vallabhbhai National Institute of Technology, Surat 395007, India; ds20ph004@phy.svnit.ac.in (D.S.);
[2] Condensed Matter Theory Group, Materials Theory Division, Department of Physics and Astronomy, Uppsala University, Box 516, 75120 Uppsala, Sweden; deobrat.singh@physics.uu.se (D.S.);
[3] Department of Physics, Indian Institute of Technology Ropar, Rupnagar 140001, Punjab, India; rajeev.ahuja@physics.uu.se (R.A.);
* Correspondence: yas@phy.svnit.ac.in (Y.S.);

Scopus Author ID 35622859800
Received: 10.01.2022; Accepted: 13.02.2022; Published: 28.03.2022

Abstract: The two-dimensional (2D) materials are highly demandable for the high charge rate in batteries. In Li-ion batteries, the 2D graphene materials are mostly well-studied. For metallic material, the physical/chemical properties can be tuned because the MXenes surface has a dangling bond according to their functional group, which provides MXenes are novel materials for batter electrochemical performance. The optimization and stability of the $Hf_3C_2F_2$ monolayer are given *ab-initio* molecular dynamics (AIMD) by the density functional theory approach. Here, the monolayer of $Hf_3C_2F_2$ has a stable structure, metallic nature, and low diffusion energy barrier shows a metal anode material for the rechargeable storage device.

Keywords: $Hf_3C_2F_2$ monolayer; structural stability; electronic properties.

1. Introduction

Batteries have been most demandable in the last few years, and large-scale applications in mobile electronics, electric grids, and e-vehicles are recent advantages for environments [1-5]. The Ion battery is most demandable. The Li-ions (LIBs) are well advanced and the most stable battery technologies, compared to others with longer charge-discharge cycles and high energy density [6–9]. Sodium-ion batteries (NIBs) are also in demand because of similar chemical properties, high storage capacity, and the most abundant material on earth, allowing Sodium to compete with Lithium. The number of experiments says that 2D material shows high capacity [10-14], low open-circuit voltage, well the stability of cycle in wich 2D MXenes experimentally synthesis in MAX phase with $M_{n+1}AX_n$ (n=1,2,3..) shows batter results in anode materials of batteries, where M is known as a transition metal group (Ti, V, Zr, Hf, etc.), A is group 13-14 elements(Si, Al, Ge, Ga, etc.) and X is Carbide or Nitraide group [15-21]. In which Ti_3C_2 reported a capacity is 410 $mAhg^{-1}$ of Li atom per 1C [22]. At the same time, Density Functional Theory (DFT) predicts 320 $mAh.g^{-1}$. After terminating a halide group (F, OH, etc.) to form a $Ti_3C_2Li_2$, here lithium capacity is majorly reduced [23]. Very recently, MXenes Hf_3C_2 synthesized by the solid solution of $Hf_3[Al(Si)]_4C_6$ and via selective etching under hydrofluoric

acid the solid solution form to $Hf_3C_2T_2$ MXenes, and results show a Hf_3C_2 showed 200 cycles, 1567 mAh cm^{-3} volumetric capacity compared to $Hf_3C_2T_2$ has 640 $mAhg^{-1}$, which suggest that Hf_3C_2 as an electrode has higher potential in batteries, specifically in power electronic applications[24]. In our work, we define the electronics properties of $Hf_3C_2F_2$ using the first principle. In which we derive the density of state of $Hf_3C_2F_2$, the band structure of $Hf_3C_2F_2$. we derive structural stability of $Hf_3C_2F_2$ at room temperature performed by ab-initio molecular dynamic (MD); with the help of the above properties, we can say that $Hf_3C_2F_2$ is better electrode material for metal-ion batteries.

2. Materials and Methods

All the calculations are done using the DFT method in the projector augmented wave (PAW) study as employed in the Vienna ab initio simulation (VASP)[25,26]. Here, for better results, we apply Perdew-Burke-Ernzerhof's (PBE) functional for relaxation of 2D $Hf_3C_2F_2$ hexagonal monolayer and explain the ion-electron exchange-correlation. In this case, the 2D MXenes relaxed with 500 eV cut-off energy without any constrains symmetry. For vacuum space in the z-axis here, we use 22.6 Å, which prevents any interaction between periodically repeated images and layers. The energy convergence for hexagonal MXenes is 10^{-6} eV, and the force is 0.003 eV/Å. For geometry optimization, the k-points are 5×5×1 with Gamma gride and 15×15×1 more significant for electronic calculations. The *ab initio* molecular dynamics were performed in 2×2×1 supercell with 5ps duration and 1 fs time step at 300K to check structural stebility[27].

3. Results and Discussion

3.1. The structural properties of MXenes monolayer.

3.1.1. Structure of $Hf_3C_2F_2$ monolayer.

Along the x-y and z-x plane view of the optimized structures of the $Hf_3C_2F_2$ monolayer is shown in Figure 1. The fluorine atom is functionalized with the Hf atom on the top of the Hf_3C_2 monolayer (Figure 1(a,b)); there are three positions of Hf-base MXenes are considered. The above structure is fully optimized with lattice constant and their positions. To form a Mxenes monolayer, the required cohesive energy of $Hf_3C_2F_2$ E_c is -51.25 eV by DFT study. It means that the $Hf_3C_2F_2$ monolayer is mechanically stable. Here, the Hf-C bond length is drawn out, which indicates the strong interaction between F and Hf atoms that shows in the top-view and bottom-view of $Hf_3C_2F_2$.

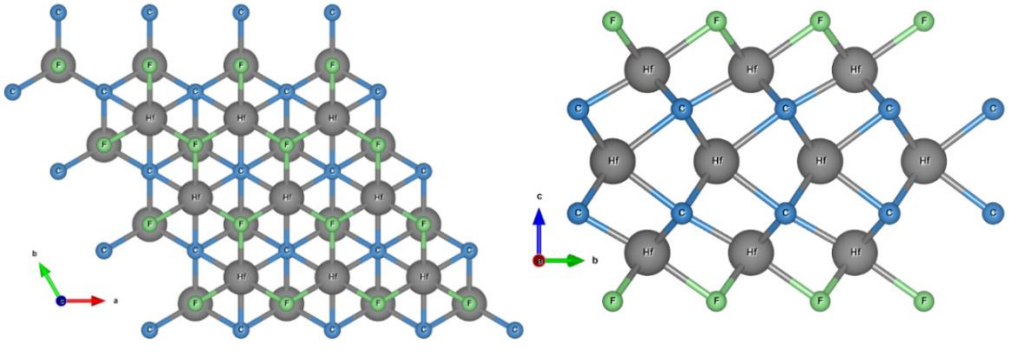

(a) **(b)**

Figure 1. (**a**) Top-view along x-y plane and (**b**) side-view along z-x plane of $Hf_3C_2F_2$ monolayer.

3.1.2. Structure dynamical properties.

The AIMD simulation was performed in a Canonical(NVT) ensemble; here, we use a 2x2x1 supercell with a time step of 1fs for a time duration of 5ps to check thermodynamic stability at room temperature. Figure 2 shows the energy convergence data as a function of time(fs) in which we put our system directly at 300 K; the results show first higher peak after time get higher energy near -257.8 eV with zig-zig form.

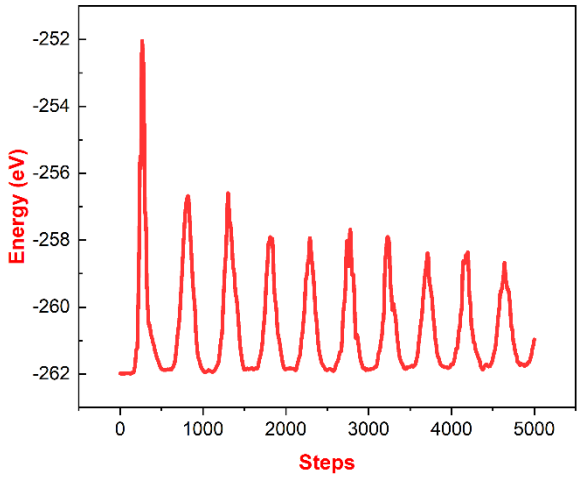

Figure 2. Shows the Energy convergence per unite time steps.

Figure 3(a), (b) show the structure at room temperature; the C atoms are slightly sifted from their positions due to vibration via temperature, but the bond between Hf-C is there, which indicates Hf-based MXenes gives experimentally positive results. Also, it was seen that there is no breaking of bonds between the atoms. From these results, we can say that the $Hf_3C_2F_2$ monolayer thermally is stable at room temperature.

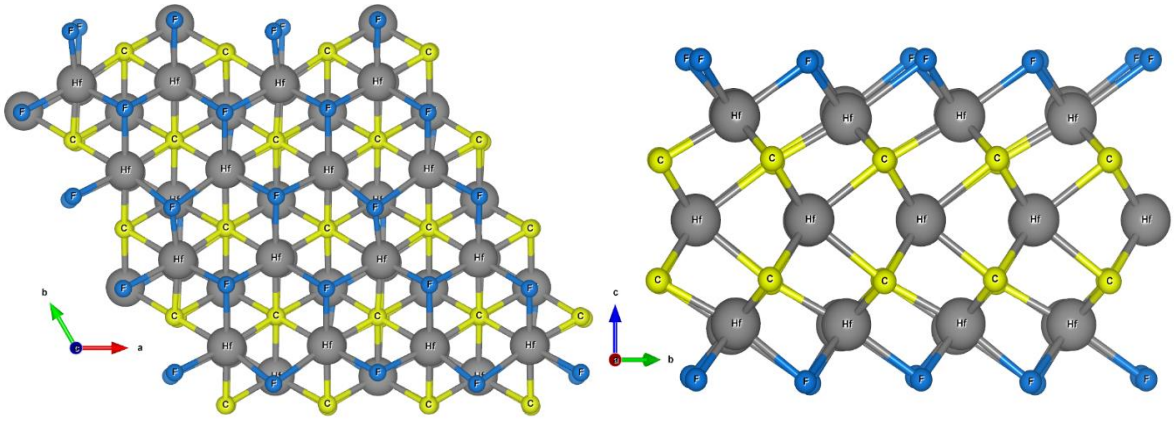

(**a**) (**b**)

Figure 3. (**a**) Top-view along the x-y plane and (**b**) side-view along the z-x plane of $Hf_3C_2F_2$ monolayer after room temperature MD.

3.2. Electronic properties and nature of $Hf_3C_2F_2$.

To understand the electronic properties of the $Hf_3C_2F_2$ monolayer, we have calculated the orbital contributed electronic band structure and projected density of states (PDOS). From the electronic properties, we discuss electrons density at different states in eV and show a more dense phase occupied by electrons. We discuss the electronic band structure, which shows the metallic nature is appropriate for anode material in metal-ion batteries.

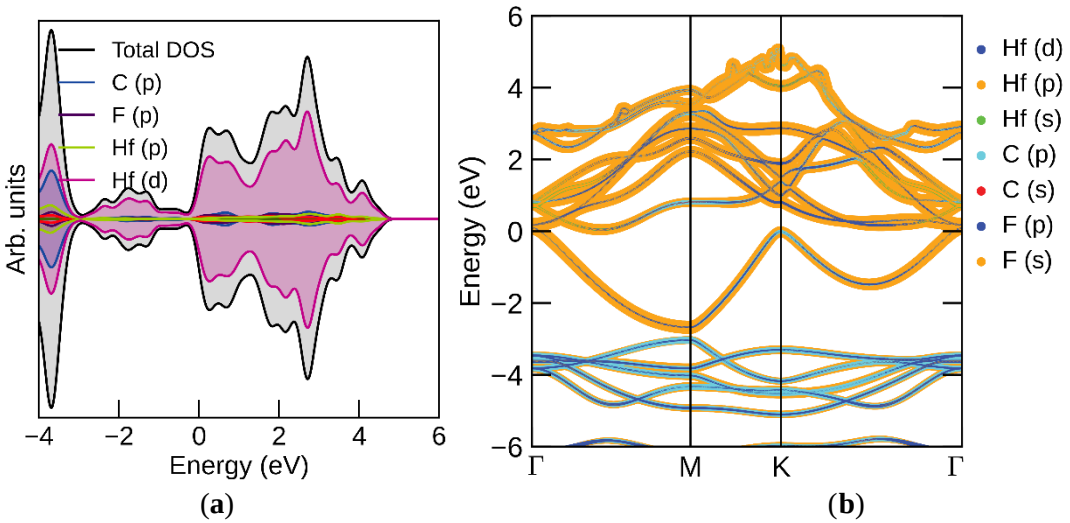

Figure 4. (**a**) the Density of states of $Hf_3C_2F_2$ and (**b**) Band structure of $Hf_3C_2F_2$.

The electronic structure of anode materials plays a vital role in the stability of the cycle and operation rate. Here, Figure 4 explains electrons' behavior per state and nature of the material. In Figure 4(a), the total DOS analysis shows the total electrons' contribution per unit state of all shells of Hf, C, and F atoms, which offer in the black line. A study of the partial DOS suggests that the Hf-d shell has more contribution in total DOS where other shells of C-p and F-p show the less contribution, F-s, and C-s shell has not contributed near the Fermi level. For material, electronic nature Figure 4(b) shows the electronic band structure of $Hf_3C_2F_2$ MXenes monolayer in which the band lines are crossing the Fermi level that implies metallic nature. From these investigations, we can say that the $Hf_3C_2F_2$ monolayer will be a better candidate for metal-ion batteries as an anode material.

4. Conclusions

We have methodically explored the structural stability electronic properties of 2D MXenes Hf3C2F2 monolayer using first-principles calculations. The 2D Mxenes $Hf_3C_2F_2$ monolayers have a favorable potential application in metal-ion batteries as an anode material because it shows metallic behavior confirmed by the DFT investigations. The $Hf_3C_2F_2$ MXenes monolayer has excellent performances, including good conductivity and stable structure by AIMD approach shows potential in energy storage application.

Funding

This research was funded by SVNIT, Surat. Fulltime Institute Research Scholar (FIR) category of registration no. DS20PH004".

Acknowledgments

For this work, the fund provided by MHRD, we thank Dr. Deobrat Singh and Prof. Rajeev Ahuja for providing kind support. We thank the team and Department of Physics, SVNIT providing a computational facility.

Conflicts of Interest

The authors declare no conflict of interest.

References

1. Dong, Y.; Shi, H.; Wu, Z. S. Recent Advances and Promise of MXene-Based Nanostructures for High-Performance Metal Ion Batteries. *Advanced Functional Materials* **2020**, *30*, 2000706, https://doi.org/10.1002/ADFM.202000706.
2. Greaves, M.; Barg, S.; Bissett, M. A. MXene-Based Anodes for Metal-Ion Batteries. *Batteries & Supercaps* **2020**, *3*, 214–235, https://doi.org/10.1002/BATT.201900165.
3. Ferrara, C.; Gentile, A.; Marchionna, S.; Ruffo, R. Ti3C2Tx MXene Compounds for Electrochemical Energy Storage. *Current Opinion in Electrochemistry* **2021**, *29*, 100764, https://doi.org/10.1016/J.COELEC.2021.100764.
4. Aslam, M. K.; AlGarni, T. S.; Javed, M. S.; Shah, S. S. A.; Hussain, S.; Xu, M. 2D MXene Materials for Sodium Ion Batteries: A Review on Energy Storage. *Journal of Energy Storage* **2021**, *37*, 102478, https://doi.org/10.1016/J.EST.2021.102478.
5. Mehta, V.; Saini, H. S.; Srivastava, S.; Kashyap, M. K.; Tankeshwar, K. Assessment of Mo2N Monolayer as Li-Ion Battery Anodes with High Cycling Stability. *Materials Today Communications* **2021**, *26*, 102100, https://doi.org/10.1016/J.MTCOMM.2021.102100.
6. Sun, M.; Schwingenschlögl, U. Structure Prototype Outperforming MXenes in Stability and Performance in Metal-Ion Batteries: A High Throughput Study. *Advanced Energy Materials* **2021**, *11*, 2003633, https://doi.org/10.1002/AENM.202003633.
7. Chen, H.; Zhang, T.; Wei, C.; Wang, J.; Niu, X. First-Principle Study of Ti2XS2 (X = C/N) MXenes as High Capacity Anodes for Rechargeable Potassium-Ion Batteries. *Applied Surface Science* **2021**, *546*, 149096, https://doi.org/10.1016/J.APSUSC.2021.149096.
8. Wyatt, B. C.; Rosenkranz, A.; Anasori, B. 2D MXenes: Tunable Mechanical and Tribological Properties. *Advanced Materials* **2021**, *33*, 2007973, https://doi.org/10.1002/ADMA.202007973.
9. Aslam, M. K.; Niu, Y.; Xu, M.; Aslam, M. K.; Xu, M.; Niu, Y. MXenes for Non-Lithium-Ion (Na, K, Ca, Mg, and Al) Batteries and Supercapacitors. *Advanced Energy Materials* **2021**, *11*, 2000681, https://doi.org/10.1002/AENM.202000681.
10. Mishra, P.; Singh, D.; Sonvane, Y.; Ahuja, R. Two-Dimensional Boron Monochalcogenide Monolayer for Thermoelectric Material. *Sustainable Energy & Fuels* **2020**, *4*, 2363–2369, https://doi.org/10.1039/D0SE00004C.
11. Mishra, P.; Singh, D.; Sonvane, Y.; Ahuja, R. Enhancement of Hydrogen Storage Capacity on Co-Functionalized GaS Monolayer under External Electric Field. *International Journal of Hydrogen Energy* **2020**, *45*, 12384–12393, https://doi.org/10.1016/J.IJHYDENE.2020.02.186.
12. Mishra, P.; Singh, D.; Sonvane, Y.; Ahuja, R. Metal-Functionalized 2D Boron Sulfide Monolayer Material Enhancing Hydrogen Storage Capacities. *Journal of Applied Physics* **2020**, *127*, 18430, https://doi.org/10.1063/5.0008980.
13. Mishra, P.; Singh, D.; Sonvane, Y.; Ahuja, R. Excitonic Effects in the Optoelectronic Properties of Graphene-like BC Monolayer. *Optical Materials* **2020**, *110*, 110476, https://doi.org/10.1016/J.OPTMAT.2020.110476.
14. Mishra, P.; Singh, D.; Sonvane, Y.; Gupta, S. K. Study of Air Stability Mechanism of 2D Boron Antimonide. *AIP Conference Proceedings* **2019**, *2142*, 110019, https://doi.org/10.1063/1.5122479.
15. Huo, X.; Wang, X.; Li, J.; Zhang, B.; Zhang, Y.; Qin, T.; Kang, F. MXenes@Te as a Composite Material for High-Performance Aluminum Batteries. *Science China Materials* **2022**, *65*, 85-94, https://doi.org/10.1007/S40843-021-1707-5.
16. Zhang, C.; Ma, Y.; Zhang, X.; Abdolhosseinzadeh, S.; Sheng, H.; Lan, W.; Pakdel, A.; Heier, J.; Nüesch, F. Two-Dimensional Transition Metal Carbides and Nitrides (MXenes): Synthesis, Properties, and Electrochemical Energy Storage Applications. *Energy & Environmental Materials* **2020**, *3*, 29–55, https://doi.org/10.1002/EEM2.12058.
17. Placke, T.; Gonzalez-Julian, J.; Bärmann, P.; Nölle, R.; Siozios, V.; Ruttert, M.; Guillon, O.; Winter, M. Solvent Co-Intercalation into Few-Layered Ti3C2Tx Mxenes in Lithium Ion Batteries Induced by Acidic or Basic Post-Treatment. *ACS Nano* **2021**, *15*, 3295–3308, https://doi.org/10.1021/ACSNANO.0C10153.
18. Luan, S.; Han, M.; Xi, Y.; Wei, K.; Wang, Y.; Zhou, J.; Hou, L.; Gao, F. MoS2-Decorated 2D Ti3C2 (MXene): A High-Performance Anode Material for Lithium-Ion Batteries. *Ionics* **2020**, *26*, 51–59, https://doi.org/10.1007/S11581-019-03182-3.
19. Ferrara C, Gentile A, Marchiona S et al.; Ti3C2Tx Mxene compounds for electrochemical energy storage. *Current opinion in Electrochemistry* **2020**, *29*, 2451-9103, https://doi.org/10.1016/J.COELEC.2021.100764.

20. Naguib, M.; Mashtalir, O.; Carle, J.; Presser, V.; Lu, J.; Hultman, L.; Gogotsi, Y.; Barsoum, M. W. Two-Dimensional Transition Metal Carbides. *ACS Nano* **2012**, *6*, 1322–1331, https://doi.org/10.1021/NN204153H.
21. Yu, T.; Zhao, Z.; Liu, L.; Zhang, S.; Xu, H.; Yang, G. TiC3 Monolayer with High Specific Capacity for Sodium-Ion Batteries. *Journal of the American Chemical Society* **2018**, *140*, 5962–5968, https://doi.org/10.1021/JACS.8B02016.
22. Yang, Z.; Zheng, Y.; Li, W.; Zhang, J. Tuning the Electrochemical Performance of Ti3C2 and Hf3C2 Monolayer by Functional Groups for Metal-Ion Battery Applications. *Nanoscale* **2021**, *13*, 11534–11543, https://doi.org/10.1039/D0NR07899A.
23. Tang, Q.; Zhou, Z.; Shen, P. Are MXenes Promising Anode Materials for Li Ion Batteries? Computational Studies on Electronic Properties and Li Storage Capability of Ti 3C 2 and Ti 3C 2X 2 (X = F, OH) Monolayer. *Journal of the American Chemical Society* **2012**, *134*, 16909–16916, https://doi.org/10.1021/JA308463R.
24. Zhou, J.; Zha, X.; Zhou, X.; Chen, F.; Gao, G.; Wang, S.; Shen, C.; Chen, T.; Zhi, C.; Eklund, P.; Du, S.; Xue, J.; Shi, W.; Chai, Z.; Huang, Q. Synthesis and Electrochemical Properties of Two-Dimensional Hafnium Carbide. *ACS Nano* **2017**, *11*, 3841–3850, https://doi.org/10.1021/ACSNANO.7B00030.
25. Kresse, G.; Furthmüller, J. Efficient Iterative Schemes for *Ab Initio* Total-Energy Calculations Using a Plane-Wave Basis Set. *Physical Review B* **1996**, *54*, 11169, https://doi.org/10.1103/PhysRevB.54.11169.
26. Blöchl, P. E. Projector Augmented-Wave Method. *Physical Review B* **1994**, *50*, 17953, https://doi.org/10.1103/PhysRevB.50.17953.
27. Martyna, G. J.; Klein, M. L.; Tuckerman, M. Nosé–Hoover Chains: The Canonical Ensemble via Continuous Dynamics. *The Journal of Chemical Physics* **1992**, *97*, 2635, https://doi.org/10.1063/1.463940.